www.differentproject.eu

Recent progresses of developing Ka Band Circular Polarizers

Emilio Arnieri , Francesco Greco, Luigi Boccia and Giandomenico Amendola

University of Calabria
Via Bucci, 42-C – Rende – Italy
emilio.arnieri@unical.it

Outline

- Introduction
- Dual-Band Converter based on a SIW Polarization Rotator
- Wide-angle Scanning Converter Based on Jerusalem-Cross FSS
- Wide-Band Dual-Frequency Converter Based on Jerusalem-Cross FSS
- Dual-Band Converter in Reflection Mode
- Conclusions

Introduction

- Over the years, many CP antenna examples have been reported in the literature;
- Polarization converters provide a valuable method to generate CP waves without affecting the complexity of the antenna system;
- Various concepts for the implementation of polarizing surfaces in both reflect and transmit mode have been presented in the last years;

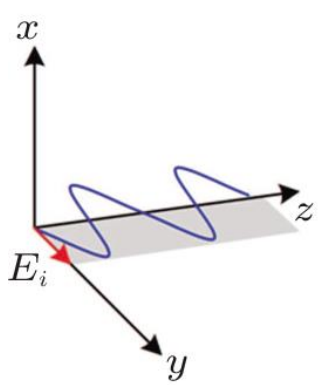

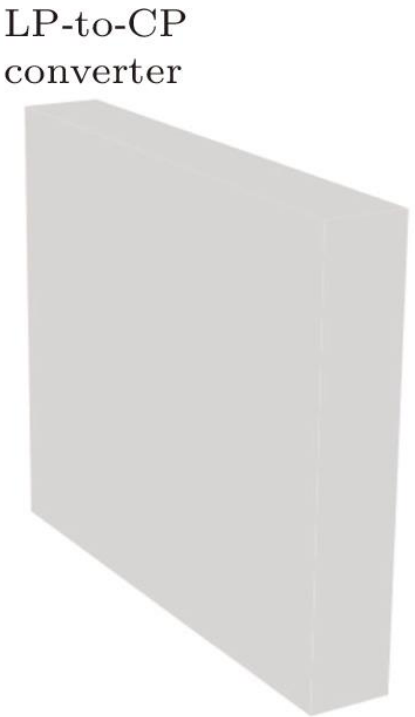

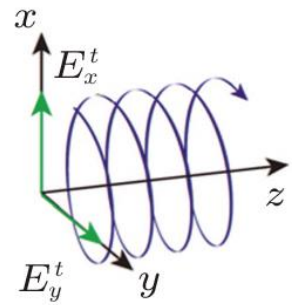

Introduction

- **Transmission-type** circular polarizers are more common and have been widely investigated in literature. In this configuration, an incoming linearly polarized wave passes through the polarizer and is transmitted like a CP wave;

- **Reflection type** circular polarizers have been also investigated in recent literature using different configurations. Dipole arrays, square lattice of helices , squares patches and array of L-patterns are examples of reflection-mode circular polarizers.

Introduction

In this presentation, we report some recent progresses of developing Ka Band Circular Polarizers at the Microwave Group of University of Calabria (Italy). Four types of LP to CP polarizers will be presented:

- A Dual-Band Converter based on a SIW Polarization Rotator;
- A Wide-angle Scanning Converter Based on Jerusalem-Cross FSS;
- A Wide-Band Dual-Frequency Converter Based on Jerusalem-Cross FSS;
- A Dual-Band Converter in Reflection Mode.

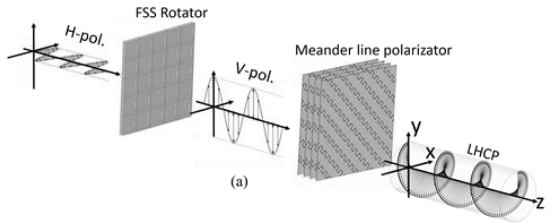

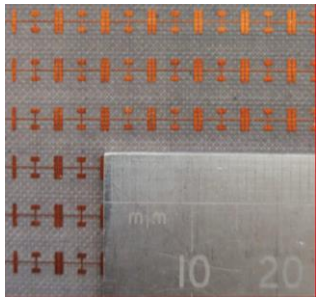

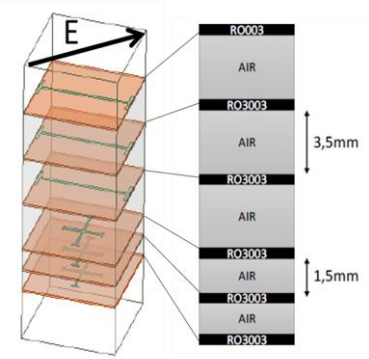

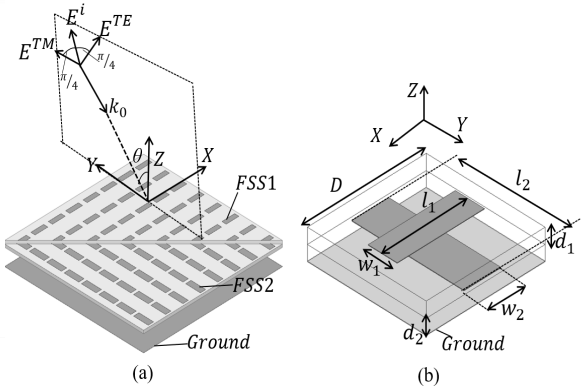

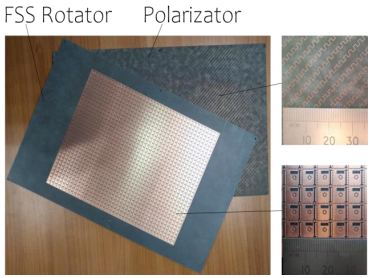

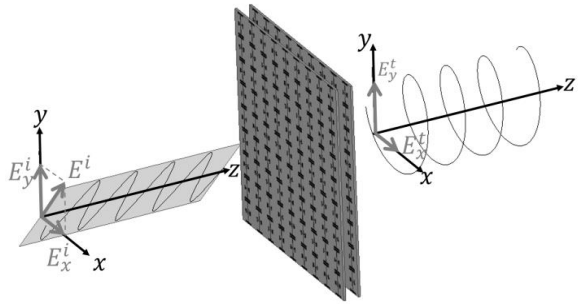

Dual-Band Converter based on a SIW Polarization Rotator

Dual-Band Converter based on a SIW Polarization Rotator

- SIW based dual-band polarization rotator optimized to selectively rotate the polarization by 90° in the K/Ka SatCom bands has been designed.

- The function of the SIW rotator is to select a linear polarization of a horizontally polarized incident wave and rotate it of 90-degree in the RX frequency band maintaining unchanged the polarization of the incident waves at the TX frequency band.

- The rotator is used in cascade with a meander line circular polarizer to achieve orthogonal circular polarizations with good axial ratio in the two bands of interest (RHCP at TX and LHCP at RX band).

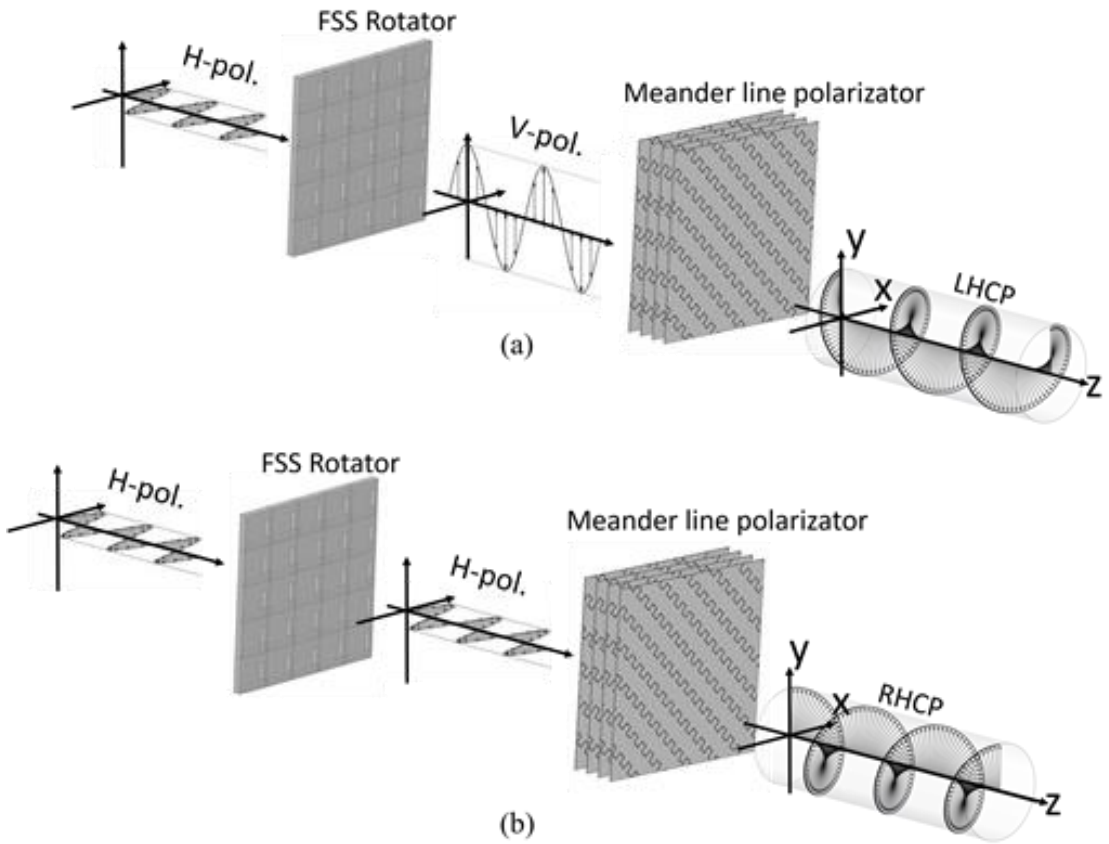

E. Arnieri, F. Greco, L. Boccia and G. Amendola, "A SIW-Based Polarization Rotator With an Application to Linear-to-Circular Dual-Band Polarizers at K-/Ka -Band," in **IEEE Transactions on Antennas and Propagation**, vol. 68, no. 5, pp. 3730-3738, May 2020, doi: 10.1109/TAP.2020.2963901.

Dual-Band Converter based on a SIW Polarization Rotator

Design of the SIW based rotator

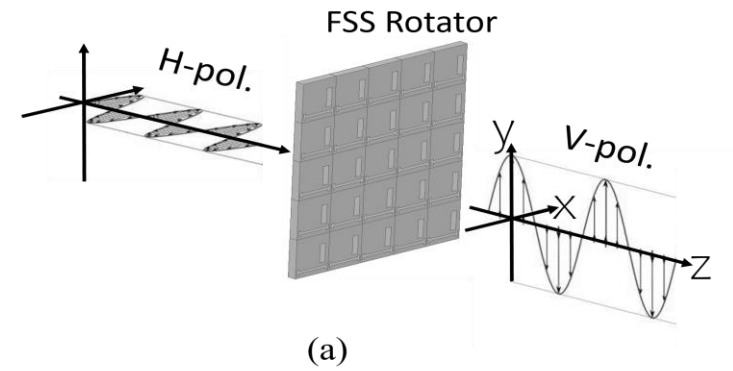

At 30 GHz the SIW cavity couples with the incoming H-polarized wave and re-radiates an outgoing H-polarized wave through the 30 GHz output slot. At 20 GHz the H-polarized wave excites the cavity through the input slot, the output 20 GHz slot is identical to the input one but is rotated of 90° and it radiates V-polarized LP wave.

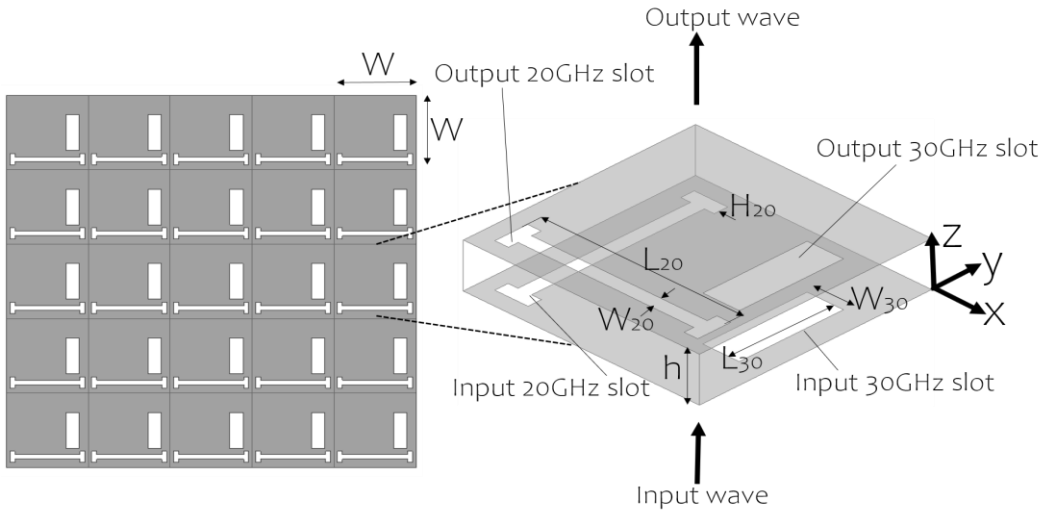

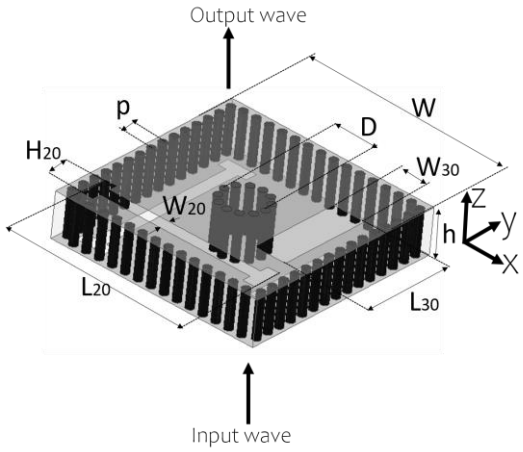

Dual-Band Converter based on a SIW Polarization Rotator

Design of the meander line polarizer

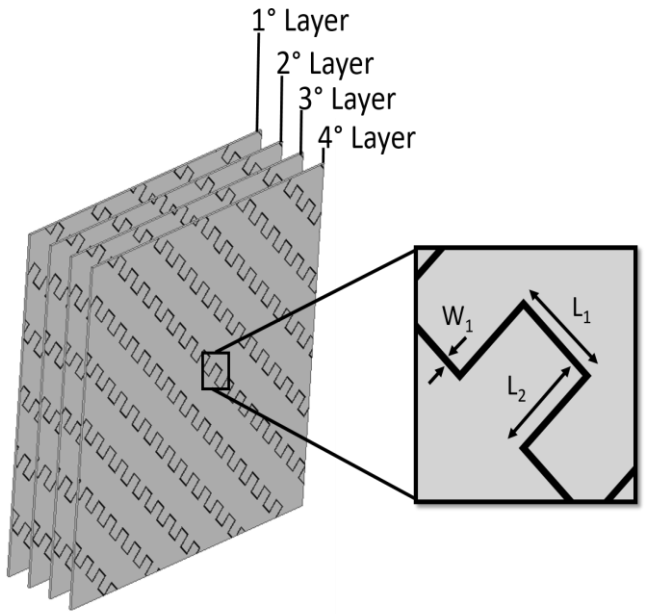

A meander polarizer is designed to cover a large bandwidth from 19 GHz to 31 GHz. Four layers of meander lines are used to obtain Circular Polarization performance over the whole bandwidth.

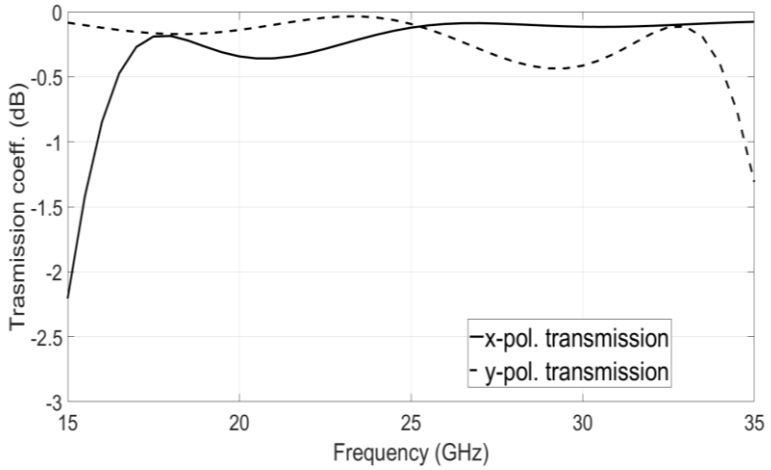

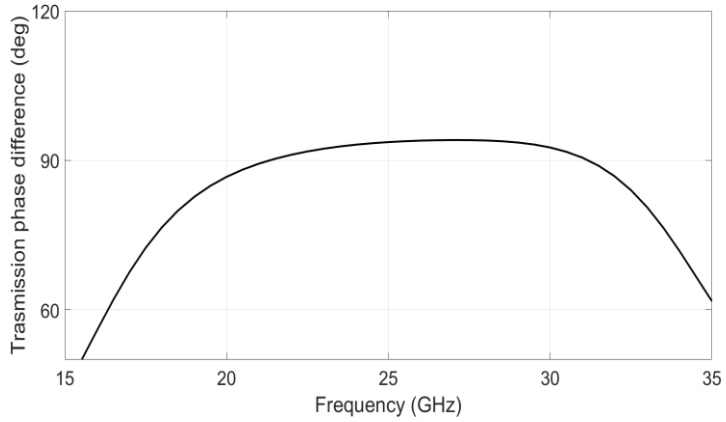

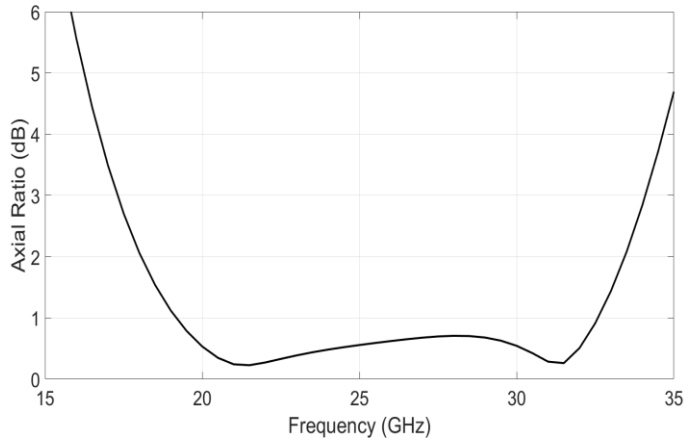

Dual-Band Converter based on a SIW Polarization Rotator

Analysis meander line and SIW rotator cascaded system

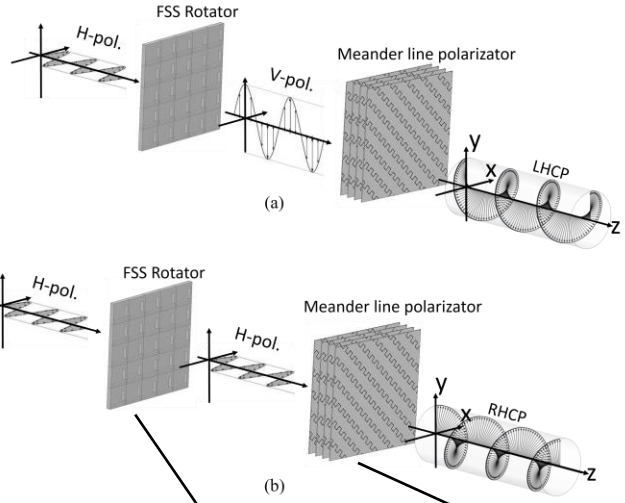

FSS Rotator Polarizator

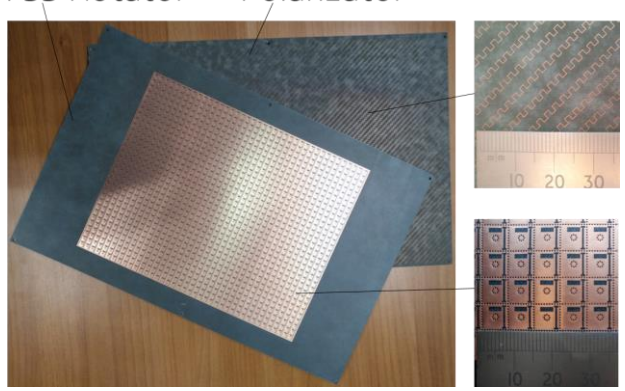

Cascaded system

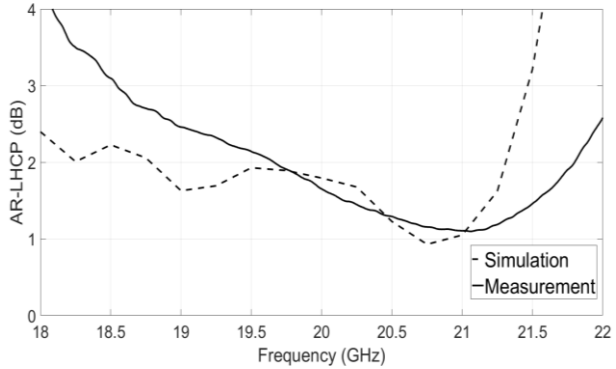

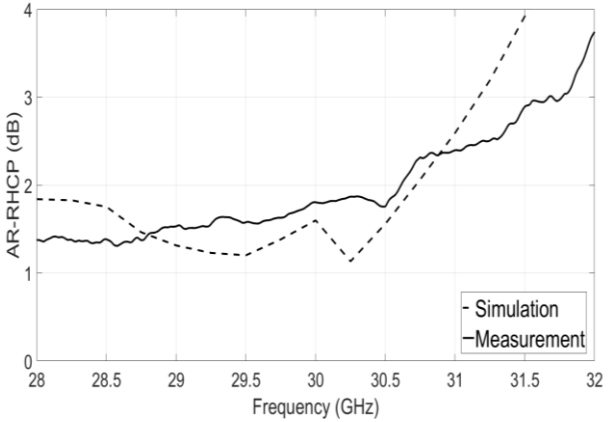

Fss Rotator

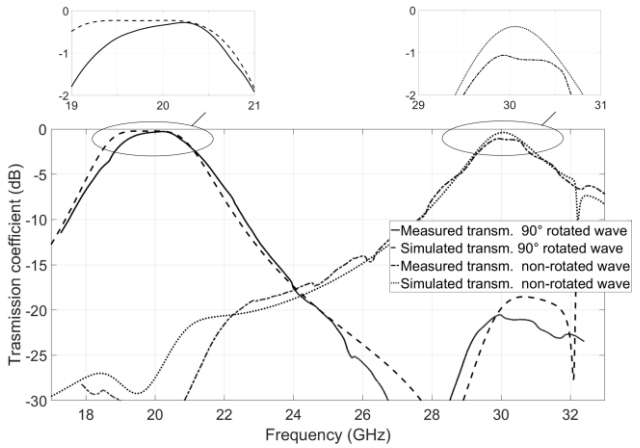

Meander line polarizator

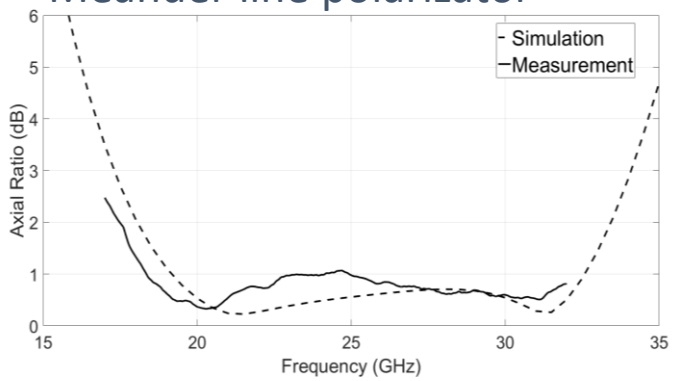

Wide-angle Scanning Converter Based on Jerusalem-Cross FSS

Wide-angle Scanning Converter Based on Jerusalem-Cross FSS

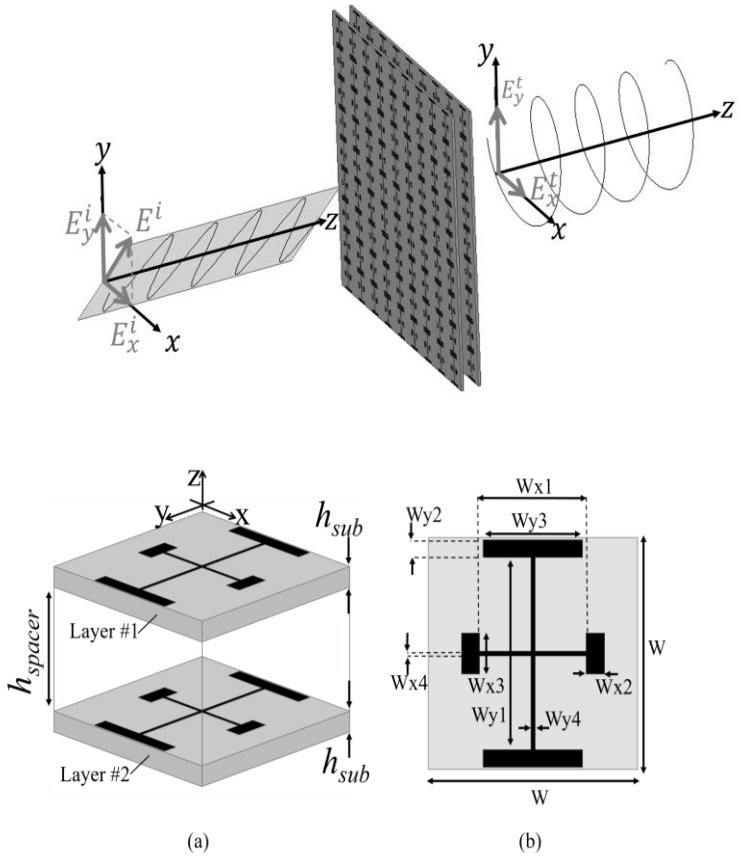

A broadband and wide-angle scanning linear-to-circular polarization converter has been designed using a dual-layer structure is presented. The elementary cell is composed of conventional Jerusalem Crosses (JC). The design procedure is based on transmission line circuit model and on full-wave simulations. The proposed equivalent circuit has been generalized to include the oblique incidence in the model. Simulated results demonstrate a 24% axial ratio bandwidth for an incidence angle θ=±50° in both x-z and y-z planes. The proposed converter provides a unique combination of wide bandwidth, thin profile, and stable response with respect to the angle of incidence. It can be integrated into any linearly polarized antenna system to generate circular polarization without significantly affecting the antenna performances.

E. Arnieri, F. Greco and G. Amendola, "A Broadband, Wide Angle Scanning, Linear to Circular Polarization Converter Based on Standard Jerusalem-Cross Frequency Selective Surfaces," **IEEE Transactions on Antennas and Propagation** (in Press).

Wide-angle Scanning Converter Based on Jerusalem-Cross FSS

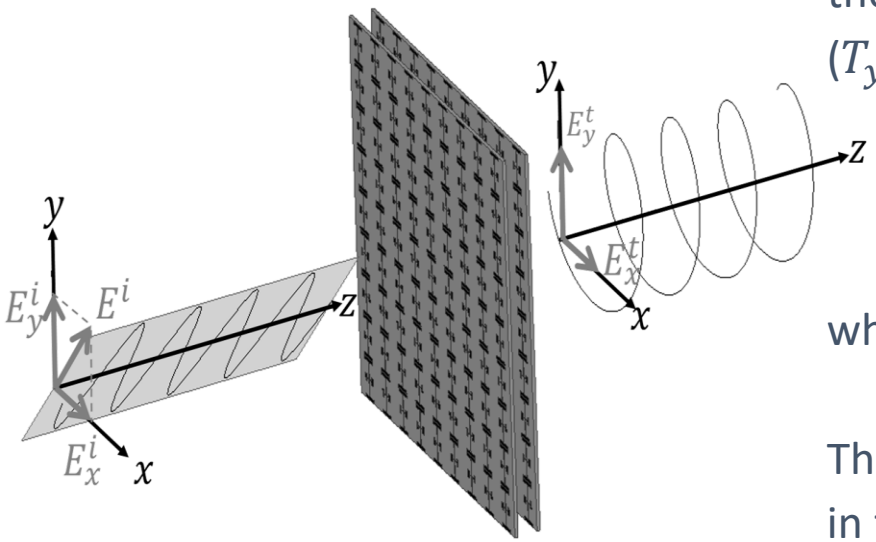

The impinging E-field is seen as composed of its horizontal $\left(E_x^i\right)$ and vertical (E_y^i) components.

The orthogonal components of the transmitted wave can be expressed using the transmission coefficients of the device for the *x* (T_x) and *y* polarizations (T_y):

$$E_x^t = T_x E_x^i; \quad E_y^t = T_y E_y^i$$

where $T_x = |T_x|e^{i\measuredangle T_x}$ and $T_y = \left|T_y\right|e^{i\measuredangle T_y}$

The circular polarization is obtained when the following conditions are fulfilled in the band of interest:

$$\measuredangle T_x = \measuredangle T_y \pm 90°$$

$$|T_x| = \left|T_y\right|$$

Wide-angle Scanning Converter Based on Jerusalem-Cross FSS

Equivalent Circuit (normal incidence)

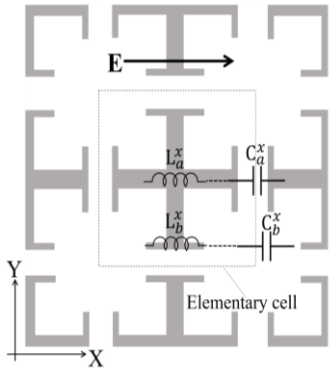

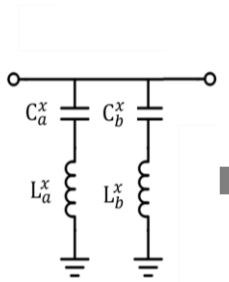

$$Z_{LC}^{p} = \frac{(1-\omega^2 L_a^p C_a^p)(1-\omega^2 L_b^p C_b^p)}{j\omega\left[C_a^p + C_b^p - \omega^2 C_a^p C_b^p (L_b^a + L_b^p)\right]}$$

where p=x or p=y

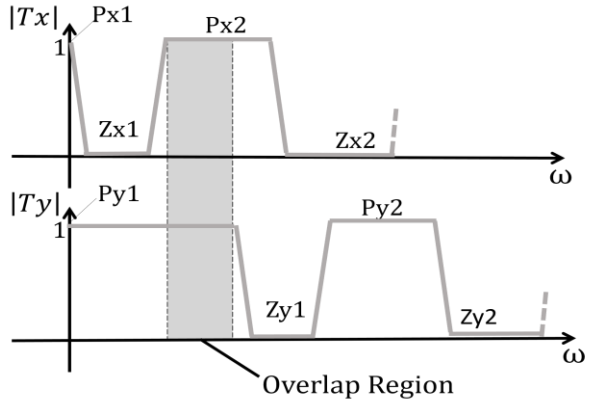

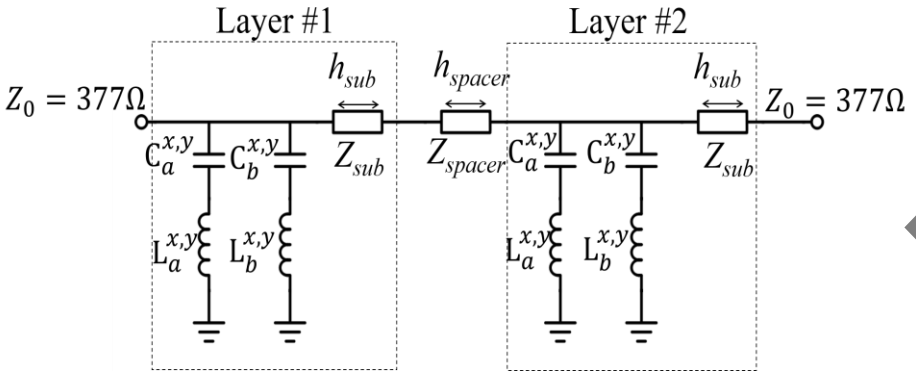

$Z_{spacer} = Z_0/\sqrt{\varepsilon_{spacer}}$, $Z_0 = 377\Omega$,
$\beta_{0spacer} = \beta_0\sqrt{\varepsilon_{spacer}}$, $\beta_0 = \omega/c$, $Z_{sub} = Z_0/\sqrt{\varepsilon_r}$
$\beta_{sub} = \beta_0\sqrt{\varepsilon_r}$.

The relation between the values of capacitances/inductances and the position of the poles and the zeros can be determined by equating to zero the numerator and the denominator of equation used to compute Z_{LC}^{p} . For the *y*-polarization case the following relations were obtained:

$$C_a^y = \frac{1}{L_a^y \omega_{zy1}^2};\ C_b^y = \frac{1}{L_b^y \omega_{zy2}^2};\qquad L_b^y = \left(\frac{\omega_{py2}^2}{\omega_{zy2}^2} L_a^y C_a^y - \frac{1}{\omega_{zy2}^2}\right) \Big/ \left[C_a^y \left(1 - \frac{\omega_{py2}^2}{\omega_{zy2}^2}\right)\right]$$

Where $\omega_{zy1}, \omega_{zy2}, \omega_{py2}$ are the frequencies of the zeros (Z_{y1} , Z_{y2}) and of the second pole (P_{y2}) for the *y*-polarization as shown in Fig.4.

Wide-angle Scanning Converter Based on Jerusalem-Cross FSS

Equivalent Circuit (oblique incidence)

The proposed equivalent circuit model was generalized to consider also the oblique incidence scenario.

$$\sin(\theta_{inc\_1}) = \sqrt{\varepsilon_r}\sin(\theta_{d1}) = \sqrt{\varepsilon_{spacer}}\sin(\theta_{inc\_2})$$

$$\beta_{sub\_i} = \beta_0\sqrt{\varepsilon_r}\cos(\theta_{di}); \quad \beta_{spacer} = \beta_{0spacer}\cos(\theta_{inc\_2})$$

$$Z_{sub\_i} = \begin{cases} Z_{sub}\sec(\theta_{inc\_i}) \text{ for } x-z \text{ incidence} \\ Z_{sub}\cos(\theta_{inc\_i}) \text{ for } y-z \text{ incidence} \end{cases}$$

$$Z_{spacer} = \begin{cases} Z_0\sec(\theta_{inc\_2}) \text{ for } x-z \text{ incidence} \\ Z_0\cos(\theta_{inc\_2}) \text{ for } y-z \text{ incidence} \end{cases}$$

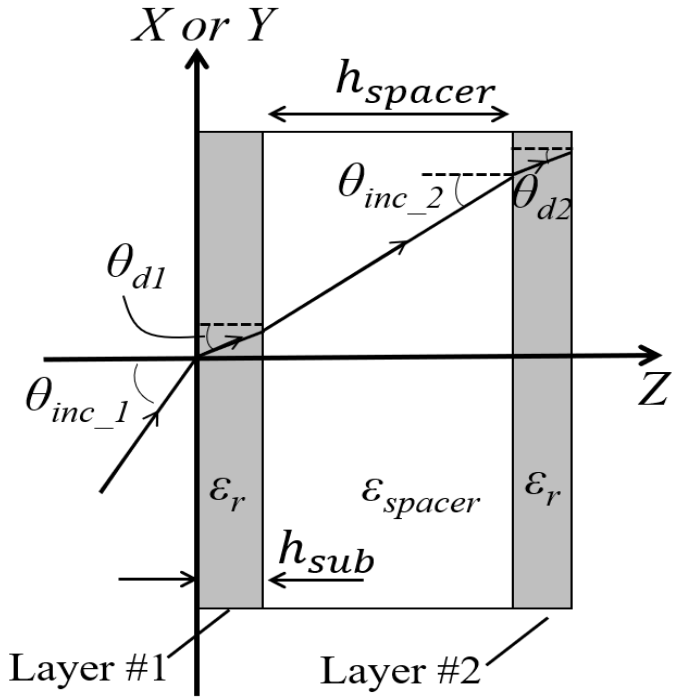

The equivalent capacitances/inductances are angle-dependent.
The following correction are used:

$$C_{a,i}^p = \begin{cases} C_a^p\left[1-\frac{\beta_0^2}{\beta_{eff,i}^2}\frac{\sin^2(\theta_{inc\_i})}{7}\right] & for\ x-z\ incid. \\ C_a^p & for\ y-z\ incid. \end{cases} \quad L_{a,i}^p = \begin{cases} L_a^p\left[1-\frac{\beta_0^2}{\beta_{eff,i}^2}\frac{\sin^2(\theta_{inc\_i})}{3}\right]^{-1} & for\ y-z\ incid. \\ L_a^p & for\ x-z\ incid. \end{cases}$$

Wide-angle Scanning Converter Based on Jerusalem-Cross FSS

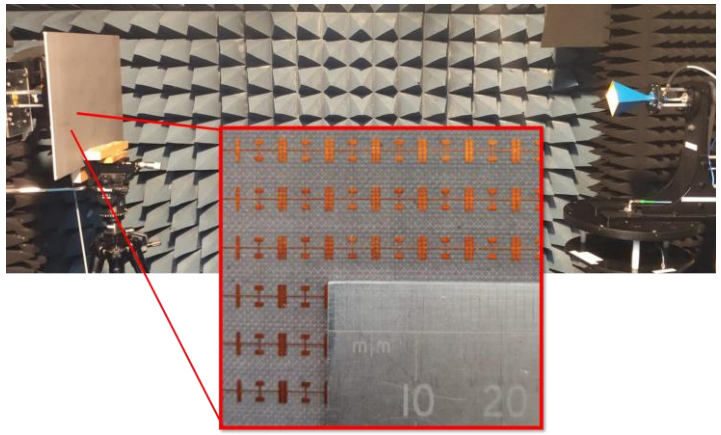

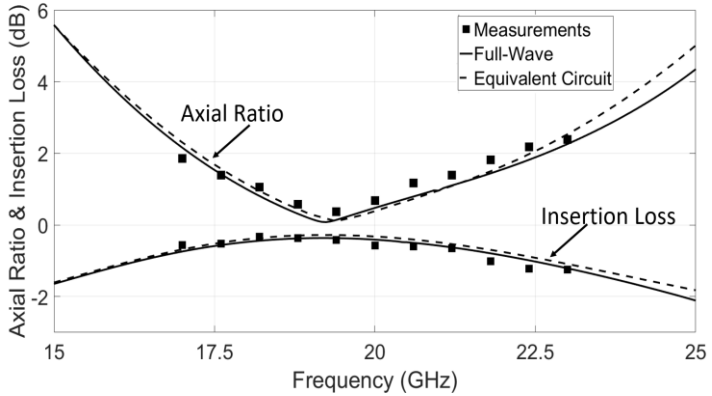

x-z plane of incidence

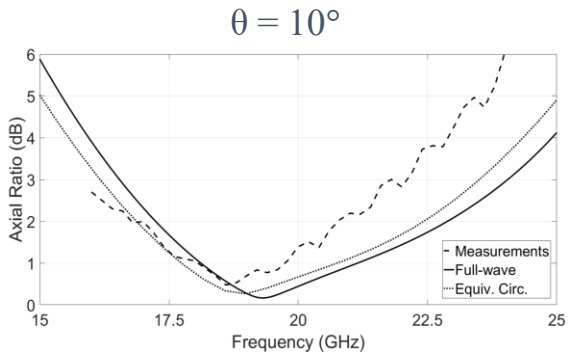

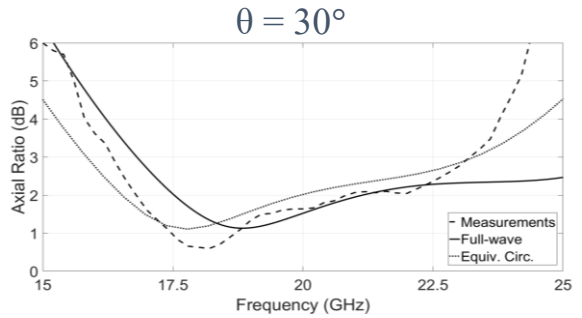

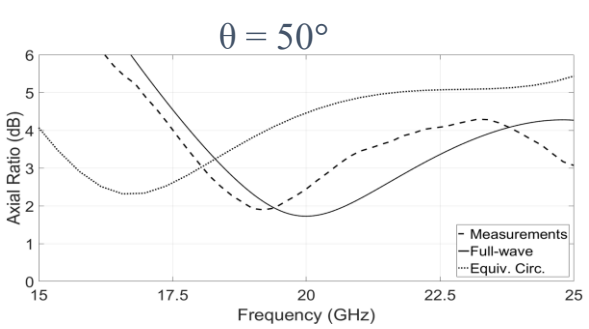

y-z plane of incidence

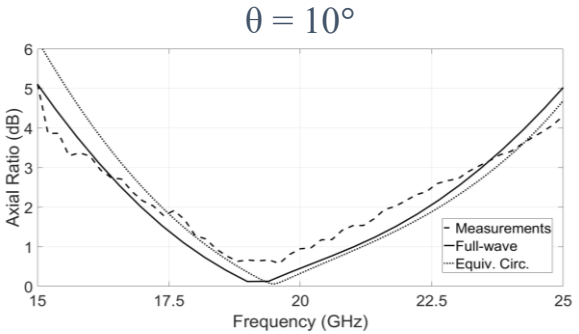

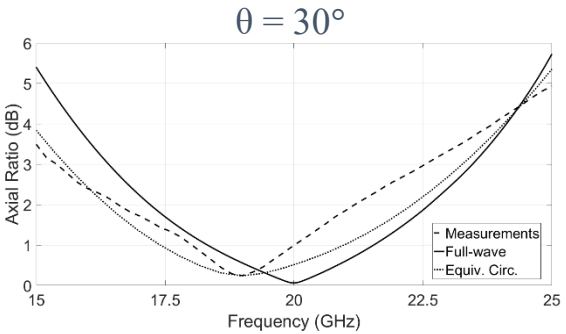

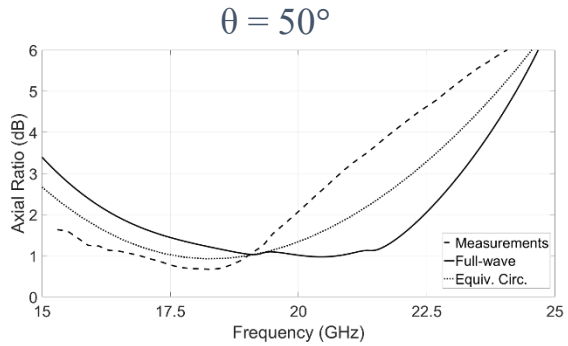

Wide-angle Scanning Converter Based on Jerusalem-Cross FSS

Performances Comparison

Ref.	Design	Central Freq. (GHz)	Cell. Size (λ)	3dB AR BW(%) *	Max IL (dB)**	Thickness	# of Layers	Angular Stability ***
[1]	Jerusalem cross & I-type dipole	18.5-29 (2-band)	0.25×0.25	29, 12	2, 0.8	1.6 mm (0.16λ)	1	±20°
[2]	Meander line	23.5	0.27×0.27	26	3	0.254 mm (0.02λ)	1	±30°
[3]	Cross and metal strips	8.48	0.42×0.42	64	<2	6 mm (0.17λ)	4	±20°
[4]	Patches and wire grids	10	0.15×0.15	40	2.7	5.4 mm (0.18λ)	4	±45°
[5]	Modified Jerusalem Cross	20	0.17×0.17	11	0.4	3.15 mm (0.21λ)	3	±30°
[6]	Meander line	29.75	0.14×0.54	12	0.5	6.5 mm (0.65λ)	4	±25°
[7]	Split ring	31	0.52×0.52	35	<0.5	8 mm (0.80λ)	4	±25°
[8]	Cross Slot	10	0.9×1.1	12	0.9	12 mm (0.40λ)	2	±20°
[9]	Zigzag metasurfaces	8.5	0.17×0.17	41	<0.8	0.508 mm (0.01λ)	1	±30°
[10]	Patch and loop	27	0.32×0.32	17.8	<0.5	6.3 mm (0.57λ)	5	±50°
This Work	**Jerusalem Cross**	**20**	**0.35×0.35**	**24**	**1.1**	**4 mm (0.27λ)**	**2**	**±50°**

*Around the central frequency; **At normal incidence; ***Relative to the 3dB AR BW.

[1]I. Sohail, Y. Ranga, K. P. Esselle, and S. G. Hay, 'A linear to circular polarization converter based on Jerusalem-Cross frequency selective surface', in *2013 7th European Conference on Antennas and Propagation (EuCAP)*, Apr. 2013, pp. 2141–2143.

[2] P. Fei, Z. Shen, X. Wen, and F. Nian, 'A Single-Layer Circular Polarizer Based on Hybrid Meander Line and Loop Configuration', *IEEE Trans. Antennas Propag.*, vol. 63, no. 10, pp. 4609–4614,

[3] W. Zhang, J. Li, and J. Xie, 'A Broadband Circular Polarizer Based on Cross-Shaped Composite Frequency Selective Surfaces', IEEE Trans. Antennas Propag., vol. 65, no. 10, pp. 5623–5627, Oct. 2017

[4] S. M. A. M. H. Abadi and N. Behdad, 'Wideband Linear-to-Circular Polarization Converters Based on Miniaturized-Element Frequency Selective Surfaces', IEEE Trans. Antennas Propag., vol. 64, no. 2, pp. 525–534, Feb. 2016

[5] M. Hosseini and S. V. Hum, 'A Circuit-Driven Design Methodology for a Circular Polarizer Based on Modified Jerusalem Cross Grids', IEEE Trans. Antennas Propag., vol. 65, no. 10, pp. 5322–5331, Oct.

[6] M. Letizia, B. Fuchs, C. Zorraquino, J.-F. Zurcher, and J. R. Mosig, 'Oblique Incidence Design of Meander-Line Polarizers for Dielectric Lens Antennas', Prog. Electromagn. Res., vol. 45, pp. 309–335, 2012

[7] L. Martinez-Lopez, J. Rodriguez-Cuevas, J. I. Martinez-Lopez, and A. E. Martynyuk, 'A Multilayer Circular Polarizer Based on Bisected Split-Ring Frequency Selective Surfaces', IEEE Antennas Wirel. Propag. Lett., vol. 13, pp. 153–156, 2014,

[8] W. Zhang, J. Li, and J. Xie, 'A Broadband Circular Polarizer Based on Cross-Shaped Composite Frequency Selective Surfaces', IEEE Trans. Antennas Propag., vol. 65, no. 10, pp. 5623–5627, Oct. 2017,

[9] J. D. Baena, S. B. Glybovski, J. P. del Risco, A. P. Slobozhanyuk, and P. A. Belov, 'Broadband and Thin Linear-to-Circular Polarizers Based on Self-Complementary Zigzag Metasurfaces', IEEE Trans. Antennas Propag., vol. 65, no. 8, pp. 4124–4133, Aug. 2017

[10] D. Blanco and R. Sauleau, 'Broadband and Broad-Angle Multilayer Polarizer Based on Hybrid Optimization Algorithm for Low-Cost Ka-Band Applications', IEEE Trans. Antennas Propag., vol. 66, no. 4, pp. 1874–1881, Apr. 2018

Wide-Band Dual-Frequency Converter Based on Jerusalem-Cross FSS

Wide-Band Dual-Frequency Converter Based on Jerusalem-Cross FSS

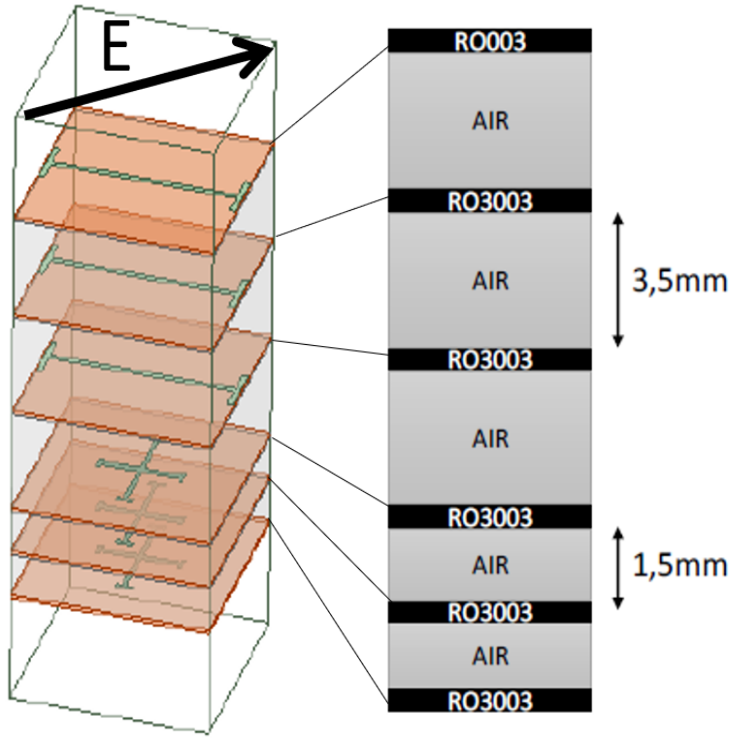

Multilayer dual band linear to circular polarization converter operating at 18.5GHz-21.5GHz (Rx band) and 28.5GHz-31GHz (Tx band).

The polarizer is composed by six metal layers printed on RO003 substrate.

The upper three layers are realized with dog bone shaped strips optimized for the Rx band.

The other layers are realized with Jerusalem Crosses, designed to convert the polarization in the Tx band

Foam spacers are used to separate the six layers.

Wide-Band Dual-Frequency Converter Based on Jerusalem-Cross FSS

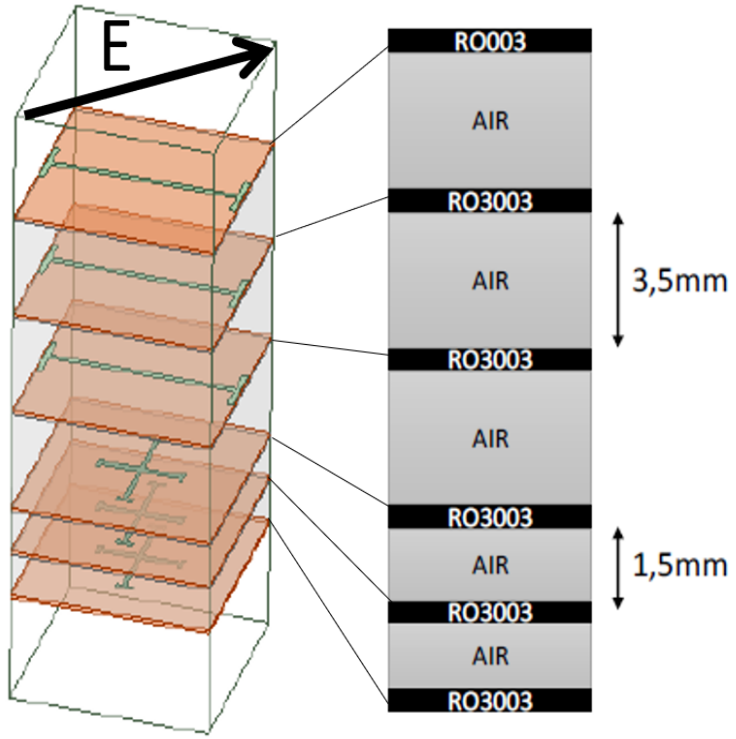

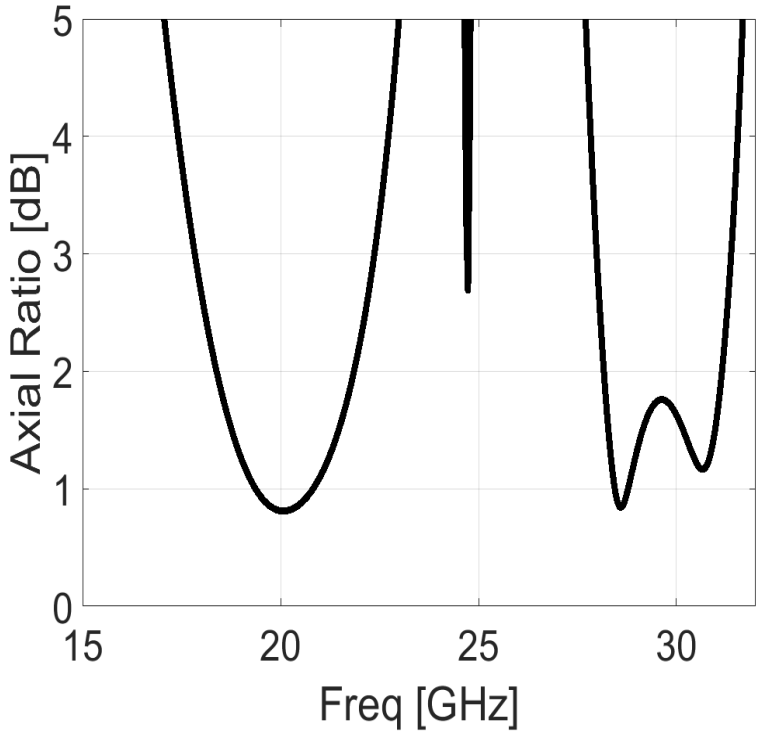

The 2dB axial ratio bandwidth is around 3.5GHz (from 18.3GHz to 21.8GHz) in RX band while around 3GHz (from 28.1GHz to 31.1GHz) in Tx band.

Dual-Band Converter in Reflection Mode

Dual-Band Converter in Reflection Mode

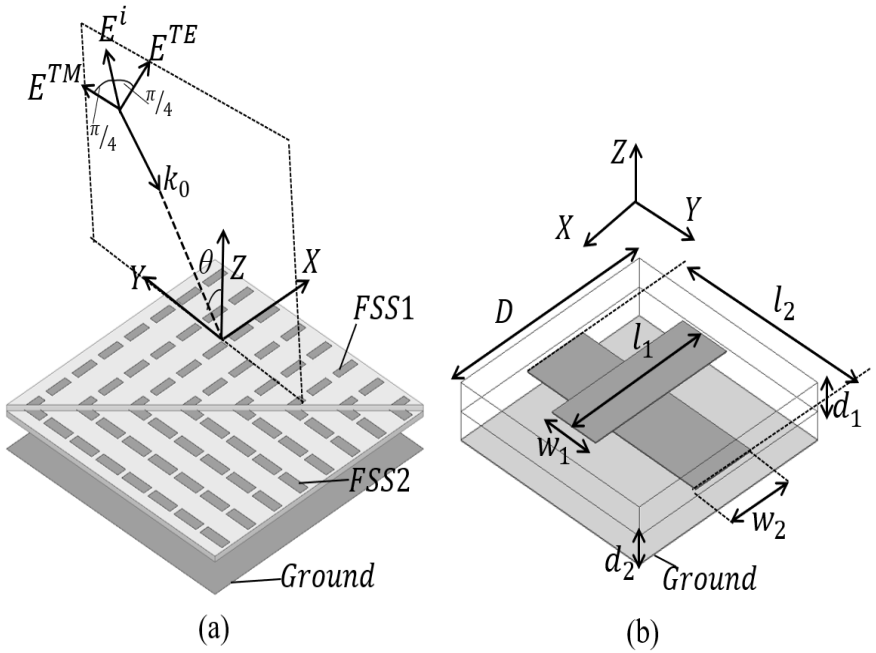

A dual band converter in reflection mode has been realized using a simple configuration composed by two orthogonal dipoles separated by a dielectric substrate.

A prototype is designed for an incident angle of $\vartheta = 30°$.

An axial ratio lower than 3dB is maintained for a wide-angle field of view of $\Delta\theta=60°$($\theta_{min} = 0°, \theta_{max} = 60°$) in two separated frequency bands where orthogonal polarizations are guaranteed.

The proposed converter can be used as sub-reflector inside a circularly polarized Cassegrain antenna system for Ka-band applications

Dual-Band Converter in Reflection Mode

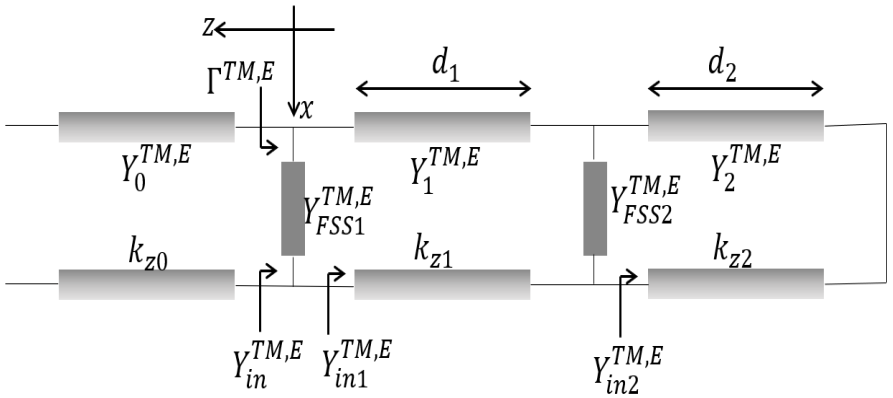

The converter has been designed using an analytic model based on a transmission lines equivalent circuit. The proposed model uses closed-form equations and can be employed to optimize the converter for a specific propagation angle θ of the incident wave. The condition to have circular polarization is:

$$\Gamma^{TE} = \mp j\Gamma^{TM}$$

$$\Gamma^{TM,E} = \frac{Y_0^{TM,E} - \left(Y_{FSS1}^{TM,E} + Y_{in1}^{TM,E}\right)}{Y_0^{TM,E} + \left(Y_{FSS1}^{TM,E} + Y_{in1}^{TM,E}\right)}$$

$$Y_{in1}^{TM,E} = Y_1^{TM,E} \frac{\frac{1}{Y_1^{TM,E}} + j\frac{\tan(k_{z1}d_1)}{Y_{FSS2}^{TM,E} + Y_{in2}^{TM,E}}}{\frac{1}{Y_{FSS2}^{TM,E} + Y_{in2}^{TM,E}} + j\frac{\tan(k_{z1}d_1)}{Y_1^{TM,E}}}$$

In a first approximation, a thin dipole can be modelled by an open circuit when illuminated with a perpendicular electric field, for this reason, we can pose $Y_{FSS1}^{TM} = Y_{FSS2}^{TE} = 0$.

Dual-Band Converter in Reflection Mode

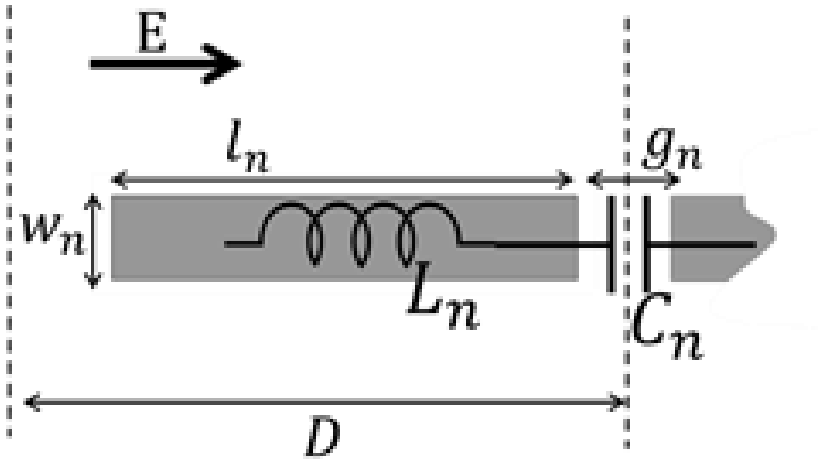

Y_{FSS1}^{TE} and Y_{FSS2}^{TM} have to be selected to satisfy the circular polarization condition in the two frequency bands

$$Y_{FSS1}^{TE} = (j\omega L_1 + 1/j\omega C_1)^{-1} \qquad Y_{FSS2}^{TM} = (j\omega L_2 + 1/j\omega C_2)^{-1}$$

Capacitances and inductances are claculated for a specifc incidence angle θ:

$$C_n(\theta_0) = \frac{2w_n}{\pi}\epsilon_0\epsilon_{eff,n}\,\mathrm{acosh}\left(\frac{D}{g_n}\right);\ n = \{1,2\}$$

$$C_n(\theta) = C_n(\theta_0)\left[1 - \frac{\sin^2(\theta)}{7\epsilon_{eff,n}}\right];\ n = \{1,2\}$$

$$L_n(\theta) = \frac{X(\theta, w_n)}{\omega}\frac{l_n}{D};\ n = \{1,2\}$$

Dual-Band Converter in Reflection Mode

Design Algorithm

The design of the linear-to-circular converter is performed for a specific angle of incidence θ following these steps:

1. The dielectric substrates are chosen including the thickness d_1 and d_2. A proper cell periodicity D is selected to avoid grating lobes. The maximum dipole length and width that can be accommodated in this cell is fixed to $l_{max} = w_{max} = D - 0.1mm$.
2. The dimension of the lower dipole $(w_2 \times l_2)$ is chosen as a starting point and the corresponding Y_{FSS2}^{TM} is computed;
3. The two required admittances ($Y_{FSS1,req}^{TE}\, RH$ and $Y_{FSS1,req}^{TE} LH$) needed to satisfy CP condition are computed in the desired bandwidth;
4. A dimension of the upper dipole $(w_1 \times l_1)$ is chosen and the corresponding Y_{FSS1}^{TE} is computed ;
5. The three parameters computed in steps 3 and 4 are plotted vs frequency. Intersection points are the frequencies were circular polarization is generated.
6. If the intersection is obtained in the two desired bands (TX and RX) the procedure is completed, otherwise, step 2-5 are repeated changing the dimensions $(w_2 \times l_2)$ and/or $(w_1 \times l_1)$ to tune the shapes of the curves and move the corresponding intersection points.

Dual-Band Converter in Reflection Mode

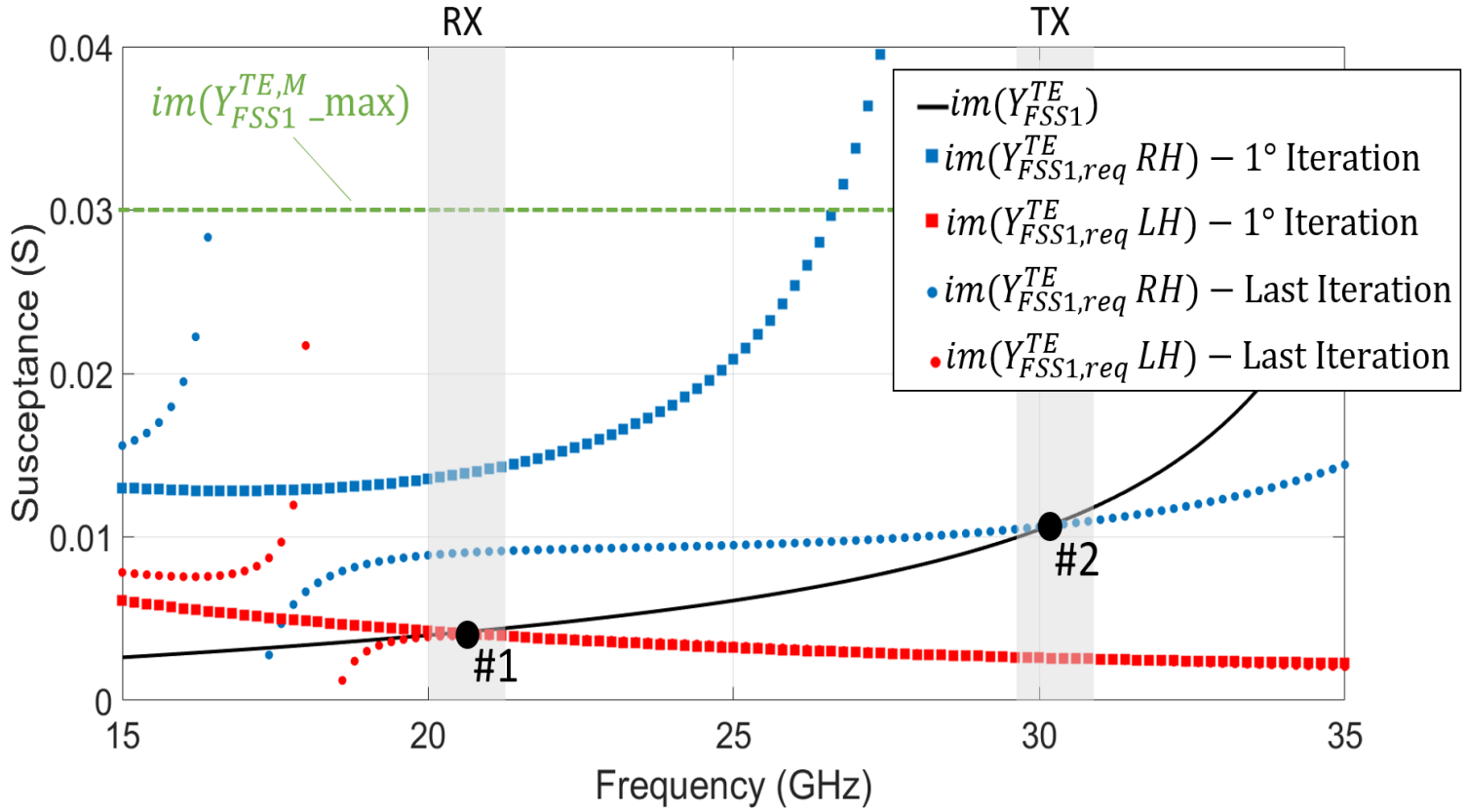

Required susceptances calculated at the first and last iteration of the proposed algorithm. Blu lines: RHCP; red lines: LHCP. Black line: susceptance of a $w_1 = 1.2mm \times l_1 = 3.48mm$ dipole printed on the top layer. Dashed green line: maximum realizable sheet susceptance. All curves are computed for an incidence angle $\theta = 30°$.

Dual-Band Converter in Reflection Mode

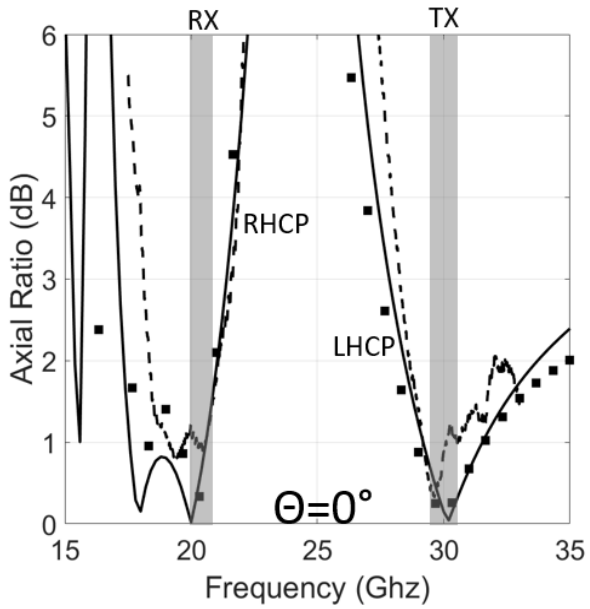

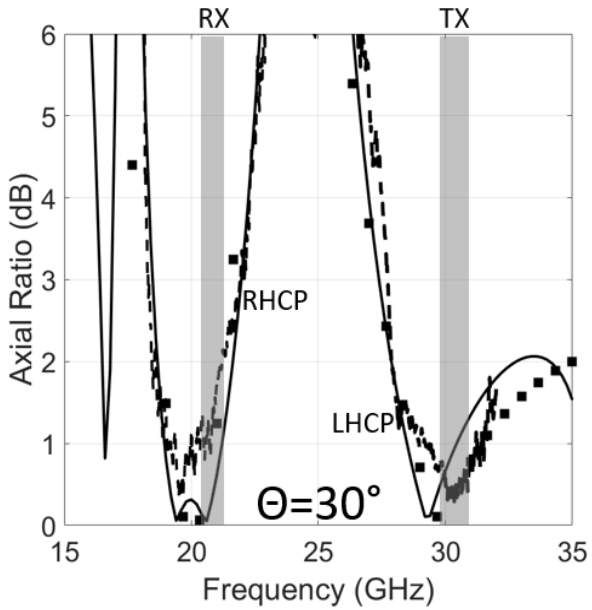

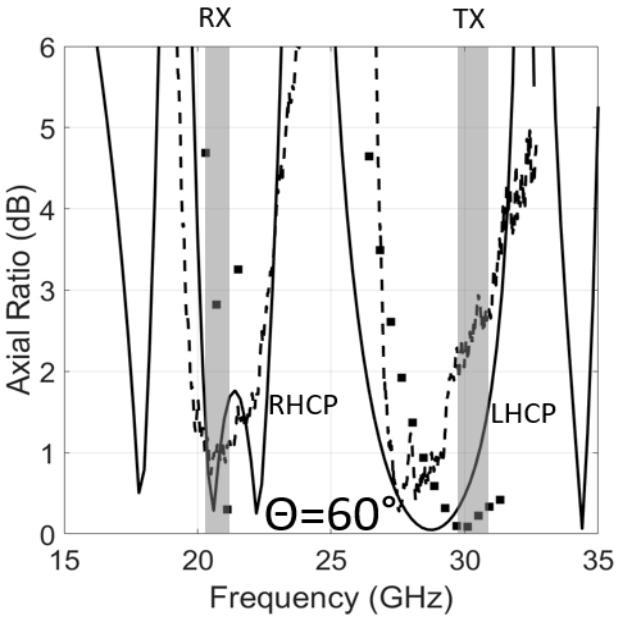

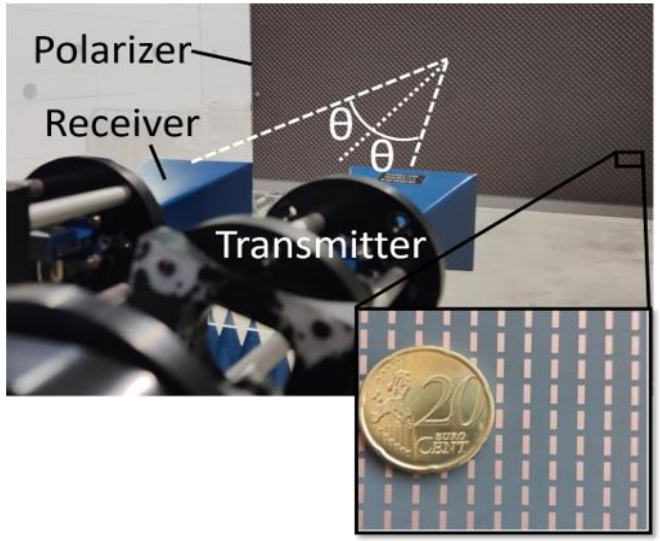

PERFORMANCE COMPARISON AMONG DUAL-BAND REFLECTION TYPE CONVERTERS

	Center Freq. (GHz)	Reflect. Loss	Dual Pol.	Angles Range ($\Delta\theta$)
[14]	2.1, 8.1	0.3 dB	Yes	14°
[15]	2.1, 8.1	0.3 dB	Yes	15°
[16]	12.1,17.7	0.2 dB	Yes	30°
[17]	20, 29.7	n/a	No	n/a
This Work	**20, 29.7**	**0.3 dB**	**Yes**	**60°**

Conclusions

- Some recent progresses of developing Ka Band Circular Polarizers at the Microwave Group of University of Calabria (Italy) have been presented.
- Four types of Linear Polarization to Circular Polarization converters including three transmission type and one reflection type are developed by using low cost standard Printed Circuit Board (PCB) technology.
- The first converter is based on a polarization rotator in SIW technology used in combination with a meander line polarizer to ensure dual band operation.
- The second converter uses a conventional JC elementary cell to provide broadband and wide-angle scanning performances.
- In the third polarizator, dog bone strips in combination with JC are used in a multilayer configuration to ensure wide-band dual-frequency behavior.
- Finally, a dual band converter in reflection mode has been developed to operate in two Ka frequency bands converting an incoming wave LP at slant 45◦ into an outgoing RHCP or LHCP wave in the Rx or Tx band respectively. The structure consists of two dipole-based FSSs separated by a dielectric substrate.
- Simulations and experiments show that good performances are obtained for all proposed solutions.